



Short communication

## C-rate performance of silicon oxycarbide anodes for Li<sup>+</sup> batteries enhanced by carbon nanotubes

J. Shen<sup>a</sup>, D. Ahn<sup>a,b,1</sup>, R. Raj<sup>a,b,\*</sup><sup>a</sup> Department of Mechanical Engineering, University of Colorado, Boulder, CO 80309-0427, United States<sup>b</sup> PDC-Energy, Louisville, CO, United States

## ARTICLE INFO

## Article history:

Received 30 September 2010

Received in revised form 2 November 2010

Accepted 2 November 2010

Available online 9 November 2010

## Keywords:

CNTs

Li ion battery anodes

Silicon oxycarbide

Polymer-derived ceramics

## ABSTRACT

We show that employing single wall carbon nanotubes (CNTs) as the conducting agent significantly increases the capacity of silicon oxycarbide anodes at high C-rates. In these anodes 515 mAh g<sup>-1</sup> can be extracted in just over 3 min. The capacity decreases to 300 mAh g<sup>-1</sup> at the same extraction rate when carbon black is used as the conducting agent. The CNT anodes have good cyclic stability, retaining 89.2% of initial capacity after 40 cycles. The coulombic efficiency ranges from 95% to 100%.

© 2010 Elsevier B.V. All rights reserved.

### 1. Introduction

High power applications of Li-ion batteries require high capacity that is accessible at high current densities. A series of anode materials have been proposed as an improvement to graphite, the conventional anode material with a theoretical specific capacity of 372 mAh g<sup>-1</sup> [1–4]. Silicon has attracted the most attention because of its very high theoretical capacity (Li<sub>4.4</sub>Si ≈ 4200 mAh g<sup>-1</sup>). However lithium insertion in bulk silicon produces a large volume change that leads to fading in just a few cycles. Efforts are underway to overcome this problem by using thin films of crystalline and amorphous silicon, and silicon-based alloys [1,5–11].

Recently a new class of materials, made from direct pyrolysis of Si-based polymers, has shown promise for anode applications. These materials, called polymer-derived-ceramics (PDCs), are constituted from Si, C and O. They show high capacity (up to 800 mAh g<sup>-1</sup>), good cyclic stability, and reasonably good C-rate performance [12]. Their performance is attributed to a nanodomain network of graphene that is embedded in tetrahedral bonds of Si, C and O [13]. The open molecular network structure of the PDCs is believed to ameliorate the large volume expansion of crystalline silicon.

In this communication, we show that the C-rate performance of SiCO is significantly enhanced if single wall carbon nanotubes

(CNTs) are employed as the conducting agent in anode formulation. The results are compared with carbon black or CAB, which is the conventional conducting agent.

### 2. Experimental

SiCO powder was synthesized from the polymer route with liquid organic precursor. 1,3,5,7-Tetramethyl-1,3,5,7-tetravinylcyclotetrasiloxane (TTCS, Gelest, PA) and dicumyl peroxide catalyst were mixed in 100:1 weight ratio and stirred until the catalyst dissolved in the liquid precursor. The solution was placed inside the vertical tube furnace (Thermolyne, IA) and cross-linked at 380 °C for 5 h under Ar gas. After the cross-linking process, the solid phase product was milled with zirconia balls as grinding media. The powders were pyrolyzed at 1000 °C for 5 h in Ar in a tube furnace (21100 Thermolyne, IA). Heating rates of cross-linking and pyrolysis procedure were 90 °C h<sup>-1</sup> and 240 °C h<sup>-1</sup>, respectively and cooling rate was same as heating rate. Upon pyrolysis, a black ceramic powder was obtained. The size of the powder particles ranged from 1 μm to 10 μm. The particles were of angular, jagged shape as would be expected from fracture and fragmentation of a glassy material. A scanning electron micrograph of the particles is shown in Fig. 1.

Elemental analysis of the SiCO powders was done for oxygen, and carbon content. Silicon content was calculated as the difference between the sum of the measured oxygen and carbon content and the total weight of the specimen. The carbon content was measured by combustion (Lecocel II HP, LECO Corp., Model C-200, USA) method with iron chip as accelerants. The oxygen content was ana-

\* Corresponding author. Tel.: +1 303 492 1029; fax: +1 303 492 3498.

E-mail address: [rishi.raj@colorado.edu](mailto:rishi.raj@colorado.edu) (R. Raj).<sup>1</sup> Present address: General Motors Corporation, Warren, MI 48090, United States.

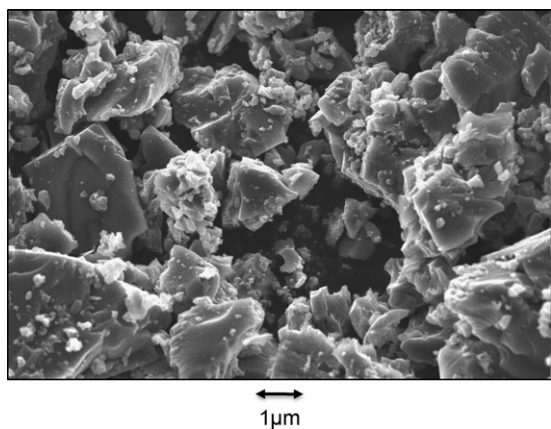


**Fig. 1.** Scanning electron micrograph of the as prepared SiCO particles, mixing with the conducting agent.

lyzed by fusion (LECO Corp., TC-600, USA) method. Cast iron with 3.36% carbon was used as standard in carbon analysis and tungsten oxide were used as the standard for oxygen analysis. In this way the composition of the SiCO powder was determined to be  $\text{SiC}_{1.98}\text{O}_{0.85}$ .

Anodes were fabricated from the SiCO powder. The powder is mixed with a conducting medium (CAB or CNT) and a polymer binder into a slurry, using the procedure described in the following paragraph. The slurry mixture is coated on a copper foil which serves as the current collector. The copper coated anode is dried at  $250^\circ\text{C}$  in an argon atmosphere to remove all solvent and moisture.

The SiCO-CAB anode is constructed by mixing 80 wt% of SiCO, 10 wt% CAB, and 10 wt% polyvinylidene fluoride (PVDF). In case of SiCO-CNT anode, 0.05 g CNT and 0.2 g SiCO are dispersed in 1500 ml,

1 wt% Triton X-100 surfactant aqueous solution by ultrasonication for 30 h. The resulting suspension is filtered through  $5\ \mu\text{m}$  pore paper. The filtered residue was heated at  $1000^\circ\text{C}$  in argon for 3 h and ground with pestle and mortar. 10 wt% of PVDF was added to this SiCO-CNT powder, which is then further processed in the same way as the SiCO-CAB anode.

The half-cell is assembled with lithium metal, polymer separator, and liquid electrolyte in the coin cell configuration. The electrolyte in these half cells is a 1 M  $\text{LiPF}_6$  solution in ethylene carbonate (EC) and dimethyl carbonate (DMC). A trilayer of polypropylene and polyethylene is used as the polymer separator (from Celgard).

The JSM-7401F field emission scanning electron microscope (JEOL, Japan) was employed to measure the microstructure of the anodes. The electrochemical experiments were carried out with a battery tester (BT-2000, Arbin Instruments). The cut-off potentials of the half cell were set between 0.01 V and 3 V. The nominal cyclic experiments were carried out with a current density of  $100\ \text{mA g}^{-1}$  in both kinds of half-cells.

### 3. Results and discussion

Scanning electron micrograph of the SiCO particles covered with CNTs is shown in Fig. 2. A careful examination of the micrograph reveals that the SiCO particles are encased in a web of CNTs, as highlighted by the sketch given on the right hand side. It is presumed that the CNTs, wrapped around the SiCO particles in this way, provided an intimate contact at the conducting agent–SiCO–electrolyte triple junctions which led to the high rate capacity as described below.

The first two Li insertion and extraction cycles for the SiCO-CAB electrode and the SiCO-CNT electrode are given in Fig. 3. These

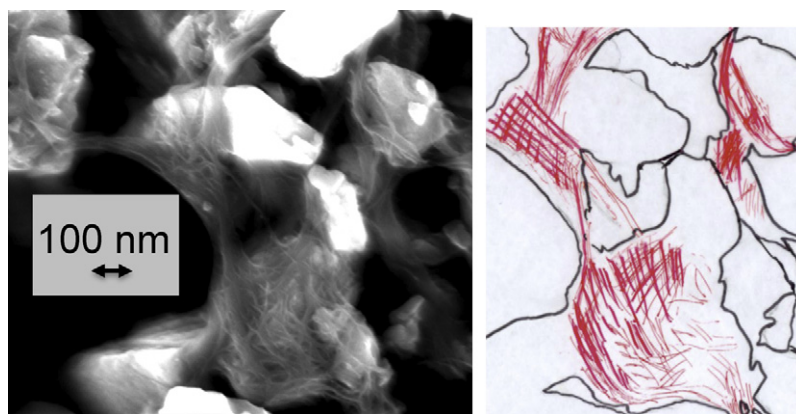


**Fig. 2.** Scanning electron micrograph of showing particles of SiCO encased in a web of CNTs, as highlighted by a hand-drawn sketch of the micrograph, given on the right.

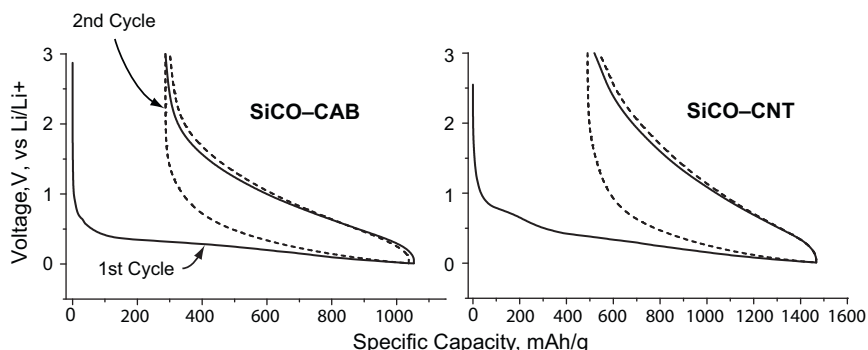


**Fig. 3.** The first two cycles of Li insertion and extraction for SiCO-CAB and SiCO-CNT anodes.

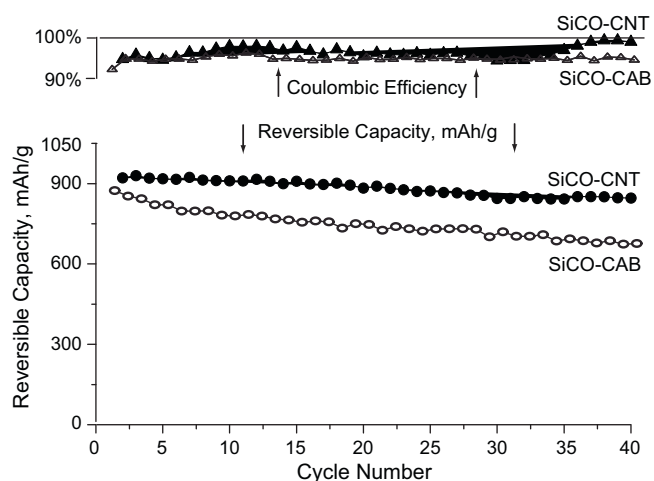


Fig. 4. Long term cyclic stability of SiCO-CAB and SiCO-CNT anodes.

data were obtained at a current density of  $100 \text{ mA g}^{-1}$  between the voltage limits of 0.01–3 V. Both electrodes show high reversible capacity. For example, in the first cycle the SiCO-CAB electrode has an insertion capacity of  $1050 \text{ mAh g}^{-1}$  of which  $767 \text{ mAh g}^{-1}$  is available reversibly in subsequent cycling, giving a first cycle loss of 27%. In the case of SiCO-CNT the corresponding values are  $1466 \text{ mAh g}^{-1}$  and  $948 \text{ mAh g}^{-1}$ , yielding a first cycle loss of 35%. In the SiCO-CNT cell a “reaction” plateau is present at about 0.8 V in the first insertion which may be related to the formation of a passivation film or solid electrolyte interphase (SEI) on the surface of the CNTs [14]. The irreversible capacity of the SiCO-CNT was slightly larger than that of SiCO-CAB electrode; this may be because, CNT by themselves have an irreversible capacity of about  $1000 \text{ mAh g}^{-1}$ , far greater than for CAB [15], natural graphite [16] and hard carbon [17]. Currently, the mechanism for irreversible insertion of lithium in polymer derived SiCO is not understood, although it has been attributed to a reaction between Li and oxygenated Si–C–O groups within the nanodomain structure of SiCO, formation of  $\text{Li}_2\text{O}$  types of bonds, and, perhaps, oxygenated functional groups on the surface of the CNT and other impurities. The formation of an SEI layer on the surface of the SiCO particles is another possible explanation for the irreversibility. The segregation of Li into nanoclusters within the SiCO molecular network is yet another possibility. For example, the higher irreversibility with carbon nanotubes may be attributed to the insertion of Li atoms within the tubular structure of the nanotubes. At the present time the molecular mechanism for irreversible sequestration of lithium is unclear; however, a mechanism similar to the filling up cylindrical pores of the CNTs with nanoclusters of Li is appealing, and would be consistent with the open molecular network structure of the PDCs: the physical density of the amorphous network is about two-thirds that of crystalline structures (silicon carbide, graphite and cristobalite) of the same overall composition.

The long term cyclic performance of cells made from SiCO-CAB and SiCO-CNT electrode is given in Fig. 4. The SiCO-CNT anodes exhibit better cyclic stability than SiCO-CAB anodes. While the SiCO-CAB electrode shows a capacity of  $630 \text{ mAh g}^{-1}$ , corresponding to 82% of the initial (reversible) capacity after 20 cycles, the SiCO-CNT electrode shows a capacity of  $846 \text{ mAh g}^{-1}$ , 89.2% of the initial charge capacity after 40 cycles. The loss of capacity with cycling may be attributed to trapping of Li within the SiCO particles, or to the growth of an SEI film from a reaction with the organic solvent and SiCO-CNT. The other factors responsible for capacity degradation with cycle-life are particle fracture and loss of electrical contact between electro-active species and the current-

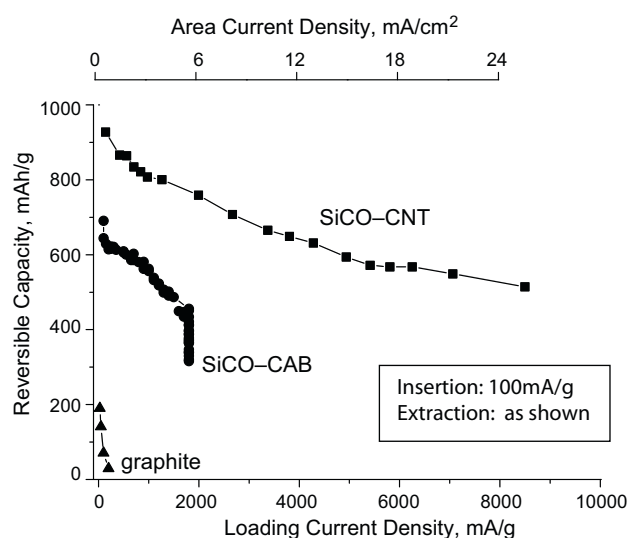


Fig. 5. Change in capacity with increasing current densities in SiCO-CNT and SiCO-CAB electrodes. Data for graphite is included for comparison. In these tests the insertion current density was held constant at  $100 \text{ mA g}^{-1}$ , while the extraction current density was varied as shown on the x-axis.

collector. The interpretation of the better cycle performance of SiCO-CNT is not yet clear but may be due to the fact that CNTs are able to maintain good electronic contact between the current collector (copper foil) and SiCO so that more active material can contribute to the capacity. It is also seen from Fig. 4 that the SiCO-CNT electrode has somewhat a more stable coulombic efficiency than the SiCO-CAB electrode.

The capacity at increasing current density for extracting Li from the anodes was measured. In these cycles, the insertion rate was kept constant at  $100 \text{ mA g}^{-1}$ , while the extraction rate was varied as shown along the x-axis in Fig. 5. Three insertion-extraction cycles were carried out at each current density. The SiCO-CNT electrode exhibited excellent rate capability: even at charge current density of  $8500 \text{ mA g}^{-1}$  (16.5C), it has an average capacity of as much as  $515 \text{ mAh g}^{-1}$ . On the other hand, the capacity of the SiCO-CAB electrode dropped rapidly when the current density was increased, yielding a capacity of only  $316 \text{ mAh g}^{-1}$  at a current density of  $1800 \text{ mA g}^{-1}$  (5.7C). Perhaps the inferior performance of the SiCO-CAB electrode can be ascribed to the low electronic conductivity of disordered carbon. However, even though the capacity of the SiCO-CAB electrode dropped quickly at high current densities, its rate capability is still better than graphite-anodes, as shown by the comparison in Fig. 5 [18,19]. It is normal for the charge capacity to decline at higher current densities. The capacity can become limited by diffusion of Li into the SiCO particles, or by the reaction at the conducting agent–SiCO–electrolyte triple junctions. The higher capacity of SiCO-CNT electrodes is ascribed to the intimate contact between the carbon nanotubes and the surface of the SiCO particles. As seen in Fig. 2 the CNTs form a web-like network around the particles. One can imagine that this fine web will maintain contact with the particle surfaces even if the particles were to suffer from fracture in high rate cycling experiments due to volume expansion.

#### 4. Conclusion

Two different anodes for Li-ion batteries, one made with carbon black (CAB) as the conducting agent and the other using CNTs as the electronic conductor were prepared and their electrochemical properties were compared. Both of them showed high storage performance. The first charge capacity of SiCO-CAB and SiCO-CNT composite were  $766.6 \text{ mAh g}^{-1}$  and  $947.5 \text{ mAh g}^{-1}$  respectively.

The cycling experiments showed that SiCO-CNT composite exhibited better long term cyclic performance than SiCO-CAB composite. After 40 cycles, the SiCO-CNT electrode exhibited a charge capacity of  $847 \text{ mAh g}^{-1}$ , 89.2% of the initial charge capacity. SiCO-CNT composite electrode also exhibited very high-rate capability. It showed an average capacity of as much as  $515 \text{ mAh g}^{-1}$  at a current density of  $8500 \text{ mA g}^{-1}$  (16.5C rate). These results point towards a high potential of SiCO-CNT as anode structures for lithium ion batteries.

### Acknowledgements

This research was supported by the Ceramics Program of the Division of Materials Research at the National Science Foundation, under Grant No: 0907108.

### References

- [1] L. Lacroic-orio, M. Tillard, D. Zitoun, C. Belin, *Chem. Mater.* 20 (2008) 1212–1214.
- [2] D. Deng, J. Yang Lee, *Chem. Mater.* 20 (2008) 1841–1846.
- [3] C.K. Chan, X.F. Zhang, Y. Cui, *Nano Lett.* 8 (2008) 307–309.
- [4] W. Zhang, J. Hu, Y. Guo, S. Zheng, L. Zhong, W. Song, L. Wan, *Adv. Mater.* 20 (2008) 1160–1165.
- [5] J. Graetz, C.C. Ahn, R. Yazami, B. Fultz, *Electrochem. Solid-State Lett.* 6 (2003) A194–197.
- [6] M. Green, E. Fielder, B. Scrosati, M. Wachtler, J.S. Moreno, *Electrochem. Solid-State Lett.* 6 (2003) A75–79.
- [7] R. Kolb, C. Fasel, V. Libau-Kunzmann, R. Riedel, *J. Eur. Ceram. Soc.* 26 (2006) 3903–3908.
- [8] Y. Hu, R. Demir-cakan, M. Titirici, J. Muller, R. Schlogl, M. Antonietti, J. Maier, *Angew. Chem. Int. Ed.* 47 (2008) 1645–1649.
- [9] T. Umeno, K. Fukuda, H. Wang, N. Dimov, T. Iwao, M. Yoshio, *Chem. Lett.* 30 (2001) 1186–1187.
- [10] I. Kim, G.E. Blomgren, P.N. Kumta, *Electrochem. Solid-State Lett.* 6 (2003) A157–161.
- [11] J. Saint, M. Morcrette, D. Larcher, L. Laffont, S. Beattie, J.P. Peres, D. Talaga, M. Couzi, J.M. Tarascon, *Adv. Funct. Mater.* 17 (2007) 1765–1774.
- [12] D. Ahn, R. Raj, *J. Power Sources* 195 (2010) 3900–3906.
- [13] A. Saha, R. Rajw, L. Don, Williamson, *J. Am. Ceram. Soc.* 89 (2006) 2188–2195.
- [14] S.H. Ng, J. Wang, Z.P. Guo, G.X. Wang, H.K. Liu, *Electrochim. Acta* 51 (2005) 23–28.
- [15] J.E.F. Agnès, S. Claye, B. Chad, Huffman, G. Andrew, Rinzler, E. Richard, Smalley, *J. Electrochem. Soc.* 147 (2000) 2845–2852.
- [16] M. Yoshio, H.Y. Wang, K. Fukuda, T. Umeno, T. Abe, Z. Ogumi, *J. Mater. Chem.* 14 (2004) 1754–1758.
- [17] W.B. Xing, J.S. Xue, T. Zheng, A. Gibaud, J.R. Dahn, *J. Electrochem. Soc.* 143 (1996) 3482–3491.
- [18] H. Buqa, D. Goers, M. Holzapfel, M.E. Spahr, P. Novaka, *J. Electrochem. Soc.* 152 (2005) A474–481.
- [19] H. Yamada, Y. Watanabe, I. Moriguchi, T. Kudo, *Solid State Ionics* 179 (2008) 1706–1709.